Dichromatic Model Based Temporal Color Constancy for AC Light Sources

Jun-Sang Yoo, Jong-Ok Kim
School of Electrical Engineering, Korea University
Seoul, Korea
look2017@korea.ac.kr, jokim@korea.ac.kr

Abstract

Existing dichromatic color constancy approach commonly requires a number of spatial pixels which have high specularity. In this paper, we propose a novel approach to estimate the illuminant chromaticity of AC light source using high-speed camera. We found that the temporal observations of an image pixel at a fixed location distribute on an identical dichromatic plane. Instead of spatial pixels with high specularity, multiple temporal samples of a pixel are exploited to determine AC pixels for dichromatic plane estimation, whose pixel intensity is sinusoidally varying well. A dichromatic plane is calculated per each AC pixel, and illuminant chromaticity is determined by the intersection of dichromatic planes. From multiple dichromatic planes, an optimal illuminant is estimated with a novel MAP framework. It is shown that the proposed method outperforms both existing dichromatic based methods and temporal color constancy methods, irrespective of the amount of specularity.

1. Introduction

Color constancy is human's inherent ability to adapt to various changes of lighting condition [30]. Thanks to our brain's memory ability, human can easily discern the original color of an object irrespective of illuminant condition [26, 29]. In contrast, for machine vision, a computational color constancy technique is necessarily required to recover the original color of an object because it does not have any prior knowledge about neither reflectance of an object nor illuminant color. Thus, color constancy plays a vital role in machine vision, which contributes to image quality enhancement. There have been many color constancy algorithms to improve color visual quality [1, 3, 7, 9, 11, 17, 34], and most of these methods are typically classified into to 4 major categories: statistics-based, physics-based, gamut-based, and learning-based methods.

Statistics-based methods have been most actively researched. Due to their simple assumption of Lambertian reflectance and low computational cost with quite high accuracy [6, 19, 39], it is even commonly used in digital camera [43]. However, there is a critical drawback of these methods that a scene must include various colors on target surfaces to satisfy their statistical assumption [10, 38, 39]. On the other hand, physics-based methods are more complex approach to color constancy than statistics-based ones in that specularity (surface reflected light) is additionally considered [36]. Their fundamental concept is based on the dichromatic reflection model, which represents the physical relationship between illuminant and object surface [13, 38]. In contrast with statistics-based methods, they work well with monotonous surface color [11, 14, 35]. However, since the number of parameters in the dichromatic reflection model is increased by adding the specular component, they become a severe ill-posed problem, and thus commonly require additional assumption such as fixed parameter (commonly diffuse weight) and sufficient specularity. Gamut-based methods [12, 16, 18] have also attracted many attentions, but they require proper training data which are appropriate for a target illuminant. Recently, there have been proposed learning-based methods to use convolutional neu-

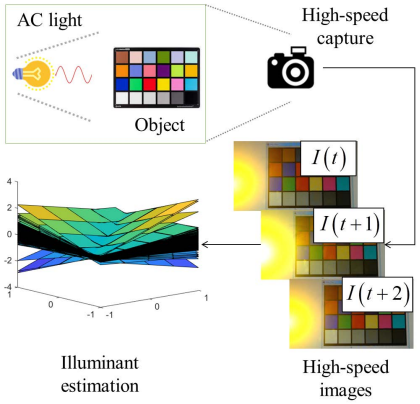

Figure 1. Summary of the proposed method. The fast variations of AC light source is captured with high-speed camera. An illuminant is estimated from multiple dichromatic planes, which are obtained from temporal observations at a pixel.

ral network. They learn the plenty of filter parameters of each layer given massive image-illuminant color pairs, and draw an optimal solution [2,4,8,21,33]. However, their performances highly depend on training data set, and still have difficulty in solving a fundamental ill-posed problem clearly such as discrimination between object reflectance and illuminant [4].

Thanks to the recent development of high-speed camera, it has been just equipped with consumer devices such as smartphone. It is expected that it will be popularly used for consumer as well as industry in future because it makes possible to capture minute variations of a scene, which is imperceptible for human eyes [5, 20]. In this paper, we propose a novel approach to exploit high-speed capture capability for color constancy. Alternative current (AC) electric power is varying sinusoidally with time. For example, it flickers 120 times per second for 60 Hz AC power. Light sources powered by this alternating current make their intensities fluctuate with an double AC frequency [44]. This flickering of AC light source can be captured by high-speed camera, and exploited as a powerful visual cue [37]. Previous dichromatic based single image methods use distinct spatial pixels to obtain a dichromatic line or a plane. Their performance significantly depends on the selection of spatial pixels (so called specular pixels), which ideally have identical diffuse and specular chromaticities. However, it is difficult to extract specular region from an image. Especially they work poorly for non-specular images, which commonly have low signal-to-noise ratio (SNR), leading to low model estimation accuracy [38, 46]. Existing dichromatic based temporal methods [31, 48] exploit the RGB intensity differences of adjacent frames to estimate illuminant color. These method also require high-specularity because a pixel with low intensity is prone to have many temporal noises.

In this paper, we propose a novel temporal color constancy method. With multiple high-speed observations at a pixel on temporal domain, it attempts to find an optimal solution for ill-posed dichromatic equation. The sinusoidal variation of AC light intensity enables us to obtain multiple distinct reflectances at the same location of a scene during a short time interval. In contrast with previous dichromatic model based methods, the proposed method does not require a high-specularity region, and does not assume that the diffuse weight of the dichromatic model is fixed. These assumptions have been a critical limitation for practical use so far. We analyzed the temporal variations of dichromatic model parameters, and actually observed that both diffuse and specular weights are dynamic under time-varying AC light. This means that under AC light sources, the dichromatic model should be described by an original plane rather than a projected line. Inspired by this observation, we first determine a set of AC pixels which are the pixels with sinusoidally varying intensity. The AC pixel is much more common than specular one, and it can be easily determined due to its periodic intensity property. Note that dichromatic based illuminant estimation is very sensitively affected by the specularity of pixel samples in existing methods. Pixel intensities on temporal domain are modeled by a sinusoidal curve using Gauss-Newton method, and a number of closely fit pixels are selected as an AC pixel. A dichromatic plane is estimated in a least-square way for each AC pixel. From those AC pixels, we obtain dichromatic planes, and a candidate illuminant is obtained by calculating the intersection of a pair of dichromatic planes. This candidate illuminant estimation is performed for all dichromatic plane pairs. Finally, an optimal illuminant is estimated by the proposed maximum a posterioi (MAP) framework. This MAP estimation is formulated by incorporating the physical and statistical properties of illuminants, which are actually directional accuracy (likelihood) and Planckian locus distance (prior constraint). Through a MAP formulation with both properties, physical and statistical advantages are optimally combined to produce an accurate estimation of illuminant.

The contributions of the paper are summarized as follows:

• Under AC illuminants, high-speed camera can capture the fast variations of illuminant intensity. We analyzed the variations of image pixel on temporal domain, and exploit them to accurately estimate a dichromatic plane, which makes it easy to estimate an optimal illuminant of a scene.

• Due to sinusoidally time-varying property of a pixel, we can easily select a AC pixel which contributes to estimate an accurate dichromatic plane. Also, it is easy to denoise it by a sinusoidal modeling. This AC pixel is easy to find and is more common than specular one.

• We propose a new MAP estimation framework to determine an optimal illuminant from multiple dichromatic planes. It incorporates the physical property and statistical prior of illuminants.

2. Dichromatic Based Illuminant Estimation

In dichromatic reflection model, reflected light from an inhomogeneous object is composed of diffuse and specular reflections, since refractive index is different between surfaces and bodies (cause diffuse reflection), and between surfaces and the air (cause specular reflection) [36]. Thus, it is composed of both diffuse and specular components, and represented by the weighted sum of chromaticity and illuminant as given by

$$I_c = m_d \Lambda_c + m_s \Gamma_c, \quad c \in r, g, b \tag{1}$$

where Λ_c and Γ_c are diffuse and illuminant (specular) chromaticitiy, respectively. In (1), m_d and m_s are diffuse and

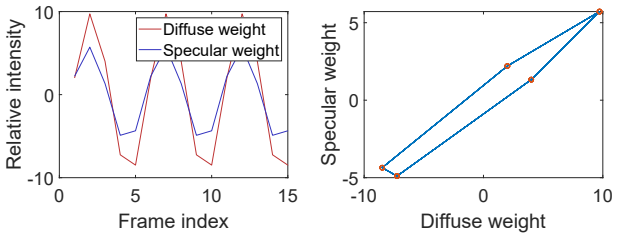

Figure 2. Variations of diffuse and specular weights. (a) Relative temporal variations and (b) their relationship. As shown in (b), m_d and m_s have a non-linear relationship, thus dichromatic model should span a plane rather than a line.

specular weights, respectively, which are defined as:

$$m_d = w_d \sum B_i, \quad m_s = w_s \sum G_i \tag{2}$$

where w_d and w_s are parameters to indicate the geometric dependence of the reflectance, and they are actually determined by the angle between surface normal and incident light direction. Both $\sum B_i$ and $\sum G_i$ are related to the intensity of incident light. Also, $\sum B_i$ and $\sum G_i$ reflect diffuse albedo and Fresnel reflectance, respectively [23, 42].

In color constancy, dichromatic model is used to separate illuminant chromaticity, Γ_c, from reflected light.

Spatial Image Color Constancy Existing dichromatic model based illuminant estimation methods can be classified into line-based [14, 25, 38, 46] and plane-based [13, 35, 40, 41] methods. In these methods, they commonly gather a group of distinct spatial pixels which are assumed to have identical Λ and Γ, and estimate multiple lines or planes for an illuminant estimation. If $m_d\left(\Lambda_c - \Gamma_c\right)$ is constant on a uniform surface, a dichromatic plane (which corresponds to (1)) can be projected into a line. In inverse intensity chromaticity (IIC) space [38], RGB chromaticity (defined as $\sigma_c = \frac{I_c}{\sum I_i}$) can be represented by linear relationship between inverse intensity of each channel and specular chromaticity, as expressed by

$$\sigma_c = p_l \frac{1}{\sum I_c} + \Gamma_c \tag{3}$$

where $p_l = m_d\left(\Lambda_c - \Gamma_c\right)$. Inspired by IIC, Woo *et al.* [46] proposed the inverse intensity red chromaticity (IIRC) space. They show that the target specular chromaticity (corresponding to Γ_c in (3)) is on the line drawn by selected specular pixels in IIRC space. These line-based methods can reduce the complexity of dichromatic model by projecting 2D plane into a 1D line. However, they commonly require so many specular pixels on uniform surfaces because m_d is assumed to be constant. In other words, if illuminant intensity varies or pixels from the surfaces with distinct geometry are selected together, they work poorly because these spatial pixels have different m_d. If pixels which have different m_d are selected, the IIC model in (3) draws a curved line rather than a straight one, and the curvedness of the dichromatic line hinders accurate illuminant estimation. Note that the direction of a dichromatic line dominantly determines illuminant color, and even a marginal error in the line direction estimation can result in large discrepancy to a ground truth illuminant. Furthermore, the direction of a dichromatic line is susceptible to noises of sample data which can severely twisted it. Dichromatic plane approaches have a similar problem with linear model because plane should be estimated from distinct spatial pixels which are assumed to have identical diffuse and specular chromaticities. It is difficult to select those pixels, and it is more complex and more sensitive to noise due to increased dimension. Thus, it has not been actively researched recently.

Temporal Image Color Constancy There have been proposed few dichromatic based temporal color constancy methods for image sequences [31, 48]. Their key concept is that m_d in (1) does not change between adjacent frames, based on the observation that incident illuminant intensity and surface geometry are usually kept unchanged on temporal domain (represented as $m_d\left(t\right) = m_d\left(t + \Delta t\right)$). Thus, by calculating the difference of pixel intensities of two neighboring frames, specular chromaticity can be estimated under the assumption that specular and diffuse chromaticity do not vary with time. This is given by

$$\Gamma_c = \frac{I_c\left(t + \Delta t\right) - I_c\left(t\right)}{m_s\left(t + \Delta t\right) - m_s\left(t\right)} = \frac{\Delta I_c\left(t\right)}{\Delta m_s\left(t\right)} \tag{4}$$

Even though $\Delta m_s\left(t\right)$ is still unknown, the specular chromaticity Γ_c can be easily calculated by normalizing $\Delta I_c\left(t\right)$. This approach is simple and has merit of fast implementation, but works poorly under less-specular because pixels in less-specular regions have relatively low SNR. Since $\Delta I_c\left(t\right)$ is commonly very small, noise can be a serious obstacle, especially for noise-prone shooting environments such as low light and high frame rate (or short exposure time), which results in low SNR.

The diffuse and specular weights in (1) are actually varying under typical indoor environments. To confirm this variations, we capture the white color checker with 150 fps. Then, diffuse and specular chromaticities are calculated from the color checker image sequence, based on the prior knowledge that the white color checker is achromatic. Dichromatic model, (1) can be re-written by the form of matrix-vector product as:

$$\begin{pmatrix} I_R \\ I_G \\ I_B \end{pmatrix} = \begin{pmatrix} \Lambda_R & \Gamma_R \\ \Lambda_G & \Gamma_G \\ \Lambda_B & \Gamma_B \end{pmatrix} \begin{pmatrix} m_d \\ m_s \end{pmatrix} \tag{5}$$

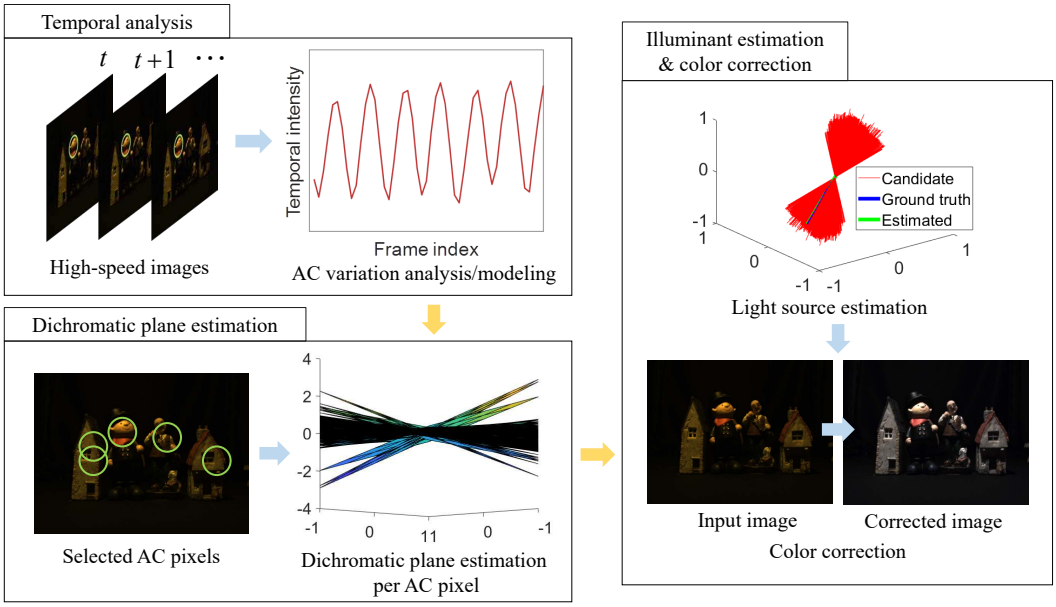

Figure 3. Summary of the proposed method. We analyzed the minute temporal intensity variations captured by high-speed image, and exploit to obtain accurate dichromatic plane for illuminant estimation.

By applying the pseudo inverse to (5), the variations of m_d and m_s can be easily estimated. As shown in Fig. 2, both m_d and m_s are dynamic because they reflect the time-varying intensity of the incident light. If geometry of image pixel also varies with time by moving light source or camera, they fluctuate more dynamically. As far as we know, these properties have been neglected so far, not being dealt with seriously. Based on this observation, the proposed method considers m_d and m_s as variable, and attempts to estimate dichromatic plane by actively exploiting time-varying AC light source.

3. The Proposed Method

Assuming static video, specular and diffuse chromaticities are kept unchanged for entire video (unless the illuminant color is changed) in dichromatic model, (1). On the other hand, the weights m_d and m_s are varying with time due to the varying intensity of AC incident light. Thus, on temporal domain, RGB intensity vectors of a fixed pixel location are exist on identical dichromatic plane (which is spanned by Λ and Γ), and their temporal locations are determined by m_d and m_s. We observe these temporal location variations of a AC pixel, and exploit it to estimate the accurate dichromatic plane. Multiple dichromatic planes are estimated from a number of AC pixels, and the illuminant color can be estimated from their intersections. However, it is challenging to estimate dichromatic plane accurately due to inherent low light noise of high-speed image caused by short exposure time. Thus, as shown in Fig. 3, we first determine a set of AC pixels, whose intensities are sinusoidally varying with time and contain much less noise. And then, dichromatic plane is estimated per AC pixel, based on its temporal intensity variations. Finally, a set of candidate illuminant vectors are extracted by calculating the intersection of each dichromatic plane pairs. The optimal illuminant is estimated using MAP estimation.

Note that the proposed method can be identically applied to dynamic video using motion estimation as [31,48]. However, it is not dealt with in our paper because estimation accuracy of dynamic video depends on the performance of motion estimation.

3.1. Selection of AC Pixel

In this subsection, we determine a number of AC pixels from input high-speed frames to estimate a dichromatic plane. An AC pixel is defined by a pixel whose intensity varies sinusoidally with time just like AC light variations. If multiple observations of a pixel on temporal domain are fit into a sinusoidal curve, it becomes an AC pixel. A high-speed image is inherently prone to noise very well due to its short exposure time. By exploiting the periodic property of an AC pixel, we can easily remove the effect of temporal noise. This noise-free AC pixel plays a vital role to estimate a dichromatic plane accurately.

The mean intensity of three RGB channels, which is expressed as $I_m = (I_R + I_G + I_B)/3$, can be modeled as sinusoidal curve with additional offset. It is represented as

$$I_m(t) \approx f(t, \boldsymbol{\beta}) = A_m \sin(4\pi f_{ac} t / f_{cam} + \phi) + \mathit{off} \quad (6)$$

where A_m is the maximum variation of AC light, ϕ is phase, f_{ac} is the frequency of AC current (*e.g.*, typically 50 or 60

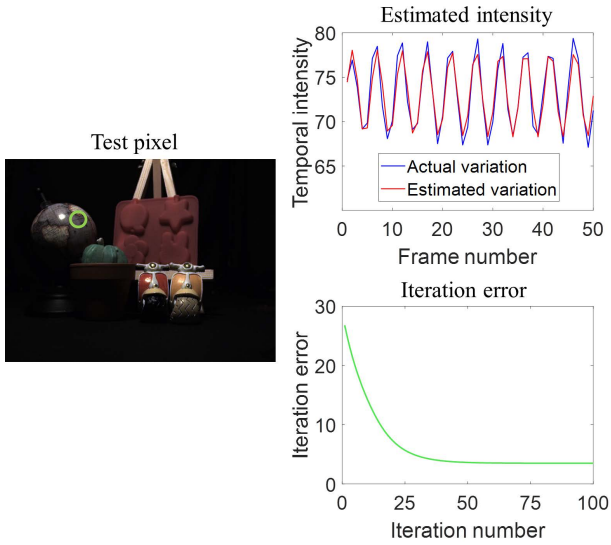

Figure 4. A sinusoidal model fit of an AC pixel. Note that iteration converges with $t < 0.03$ seconds.

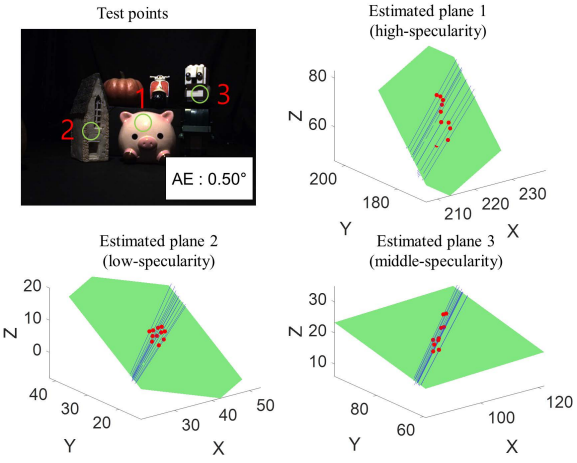

Figure 5. Examples of plane estimation. For temporal observations of the three test pixels (denoted by green circle) in the top-left image, their dichromatic planes (green plane in the plot) are estimated. Blue line denotes a RGB direction of each temporal sample. Irrespective of the extent of specularity, a dichromatic plane is estimated well in that it contains most of blue lines.

Hz), f_{cam} is capture frame rate, and *off* is a DC offset. $\boldsymbol{\beta}$ is a collection of parameters in (6), and is a parameter vector which is given by $\boldsymbol{\beta} = \begin{pmatrix} A_m & \phi & off \end{pmatrix}^{\mathsf{T}}$. Since $f(t, \boldsymbol{\beta})$ is a nonlinear function of t, $\boldsymbol{\beta}$ can be iteratively estimated using Gauss-Newton method. Gauss-Newton method is used to find a minimum of a non-linear function, and has an advantage in computation complexity because it does not require second or higher order derivatives [45].

In our work, we aim to minimize the squared error between $I_m(t)$ and $f(t, \boldsymbol{\beta})$, which is represented by $\mathbf{r}(\boldsymbol{\beta})$. Thus, we select a $\boldsymbol{\beta}$ which minimize the squared error $\mathbf{r}(\boldsymbol{\beta})^{\mathsf{T}} \mathbf{r}(\boldsymbol{\beta})$ as

$$\hat{\boldsymbol{\beta}} = \underset{\boldsymbol{\beta}}{\operatorname{argmin}} \, \mathbf{r}(\boldsymbol{\beta})^{\mathsf{T}} \mathbf{r}(\boldsymbol{\beta}) = \underset{\boldsymbol{\beta}}{\operatorname{argmin}} \sum_{t=t_1}^{t_N} \left(I_m(t) - f(t, \boldsymbol{\beta}) \right)^2 \tag{7}$$

where $\mathbf{r}$ is an error vector between $I_m(t)$ and $f(t, \boldsymbol{\beta})$ from t=t_1 to t_N. It is given by

$$\mathbf{r}(\boldsymbol{\beta}) = \begin{pmatrix} I_m(t_1) - f(t_1, \boldsymbol{\beta}) \\ \vdots \\ I_m(t_N) - f(t_N, \boldsymbol{\beta}) \end{pmatrix} \tag{8}$$

The parameter vector $\boldsymbol{\beta}$ is iterativey updated by minimizing $\mathbf{r}^{\mathsf{T}}\mathbf{r}$ as shown in right-bottom graph in Fig. 4. In our diverse experiments, $\boldsymbol{\beta}$ converges as fast as within 60 iterations.

Finally, the temporal error of a pixel is calculated to determine a AC pixel for dichromatic plane estimation.

$$E_T = \frac{\mathbf{r}\left(\hat{\boldsymbol{\beta}}\right)^{\mathsf{T}} \mathbf{r}\left(\hat{\boldsymbol{\beta}}\right)}{\hat{\boldsymbol{\beta}}(1)\, t_N} \tag{9}$$

where $\hat{\boldsymbol{\beta}}(1)$ denote the first element of $\hat{\boldsymbol{\beta}}$.

Note that the model fit error in (9) should be normalized by the estimated sinusoidal amplitude for fair comparison irrespective of pixel intensity. These AC pixels can be denoised easily and accurately with a sinusoidal model, and it can contribute to estimate more accurate dichromatic plane. It is enough to guarantee that multiple observations of an AC pixel are from the same surface (or reflectance). Thus, it does not require any specularity on a pixel. Note that AC pixels are automatically determined from an input image by choosing a pixel with low fitting error of (9).

3.2. Estimation of Dichromatic Plane

In previous subsection, a number of AC pixels are determined, and each AC pixel has N different observations at distinct time. A dichromatic plane is estimated from these N temporal observations for a given AC pixel (see Fig. 5). For k-th AC pixel, its N observed RGB pixels are on the same plane, P_k, based on the dichromatic model. If the RGB values of an AC pixel are denoted as x, y, z, the dichromatic plane P_k is expressed by

$$P_k : a_k x + b_k y + c_k = z \tag{10}$$

where $\mathbf{v}_k = \begin{pmatrix} a_k & b_k & c_k \end{pmatrix}^{\mathsf{T}}$ denotes the normal vector of the dichromatic plane P_k.

To estimate the dichromatic plane, normal vector $\mathbf{v}_k$ should be first determined optimally as follows:

$$\hat{\mathbf{v}}_k = \underset{\mathbf{v}_k}{\operatorname{argmin}} \sum_{t=t_1}^{t_N} \left(z_t - (a_k x_t + b_k y_t + c_k) \right)^2 \tag{11}$$

Figure 6. An test images extracted from videos in our laboratory setting.

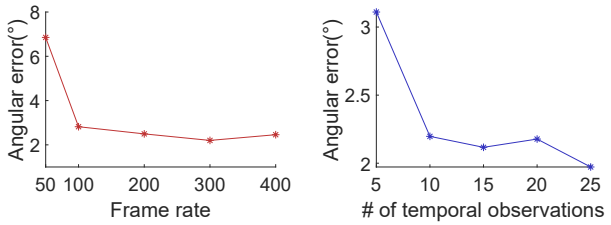

(a) (b)

Figure 7. Angular error accuracy of the proposed method with (a) various FPS and (b) number of temporal observations (150 fps).

where $\hat{\mathbf{v}}_k$ is an optimal solution to be best-fit. Its least-square solution, is given by

$$\hat{\mathbf{v}} = \left(\mathbf{A}^{\mathsf{T}}\mathbf{A}\right)^{-1}\mathbf{A}^{\mathsf{T}}\mathbf{b} \tag{12}$$

where $\mathbf{A}$ and $\mathbf{b}$ are composed of temporal observations of RGB intensities, and are given by

$$\mathbf{A} = \begin{pmatrix} x_{t_1} & y_{t_1} & 1 \\ x_{t_2} & y_{t_2} & 1 \\ & \vdots & \\ x_{t_N} & y_{t_N} & 1 \end{pmatrix} \quad \mathbf{b} = \begin{pmatrix} z_{t_1} \\ z_{t_2} \\ \vdots \\ z_{t_N} \end{pmatrix} \tag{13}$$

Then, the k-th plane error is calculated as

$$E_{P,k} = \frac{1}{I_m t_N}\left(\mathbf{A}\hat{\mathbf{v}}_k - \mathbf{b}\right)^{\mathsf{T}}\left(\mathbf{A}\hat{\mathbf{v}}_k - \mathbf{b}\right) \tag{14}$$

Note that in (14), least-square error is divided by mean intensity I_m, to neglect the intensity level of a pixel. We discard the planes which have high E_P, because they are likely to have many noises.

3.3. Illuminant Estimation

Using the plane error measured of (14), N_p accurate dichromatic planes are selected among multiple candidates. Note that a single dichromatic plane is derived per each AC pixel. Theoretically, all dichromatic planes should share a common intersection. However, all dichromatic planes may not meet at a fixed point actually due to noise and the accuracy of dichromatic model. Thus, we first calculate an intersection for a pair of dichromatic planes, and this is for all combinations, ${}_{N_p}C_2$. In other words, ${}_{N_p}C_2$ number of candidate illuminants is estimated. In this subsection, we propose a Bayesian framework to determine an optimal illuminant from ${}_{N_p}C_2$ intersections.

To obtain an optimal illuminant from dichromatic planes, we adopts a MAP. Given all estimated planes, $\mathbf{P}$, the optimal illuminant should maximize the posteriori probability $p(\Gamma|\mathbf{P})$, and posteriori probability can be decomposed into the product of likelihood and prior probability as

$$\hat{\Gamma} = \underset{\Gamma}{\operatorname{argmax}}\, p(\Gamma|\mathbf{P}) = \underset{\Gamma}{\operatorname{argmax}} \prod_{k=1}^{N_p} p(P_k|\Gamma)\, p(\Gamma) \tag{15}$$

Since all dichromatic planes estimated for an input scene should share a common illuminant vector, Γ, we can obtain the illuminant by calculating the intersection of dichromatic planes. In our work, an optimal illuminant is estimated from N_L (which is equal to ${}_{N_p}C_2$) plausible candidate illuminants. Then, (15) can be re-written as

$$\hat{\Gamma} = \underset{\Gamma_i \in \left\{\Gamma_1, \Gamma_2, \cdots, \Gamma_{N_L}\right\}}{\operatorname{argmax}} \prod_{k=1}^{N_p} p(P_k|\Gamma_i)\, p(\Gamma_i) \tag{16}$$

Taking logarithm to the right side of (16), it is rewritten by:

$$\hat{\Gamma} = \underset{\Gamma_i \in \left\{\Gamma_1, \Gamma_2, \cdots, \Gamma_{N_L}\right\}}{\operatorname{argmax}} \sum_{k=1}^{N_p} \ln p(P_k|\Gamma_i) + N_p \ln p(\Gamma_i) \tag{17}$$

$\hat{\Gamma}$ is estimated by maximizing the posterior probability of the illuminant Γ given multiple observations of dichromatic planes. Inspired by the previous combinational methods which exploit both physical and statistical properties [34, 35], the proposed framework includes both properties.

For likelihood probability, it should reflect the relationship between candidate illuminant and the plane. Given Γ_i, the accuracy of k-th plane P_k can be measured by the angle between Γ_i and the normal vector of a chromatic plane, v_k. Ideally, both directions should be orthogonal, and their angular error is converted into the probability as follows

$$p(P_k|\Gamma_i) = \exp\left(-\frac{1}{E_{p,k}}\cos\left(\frac{\hat{\mathbf{v}}_k \cdot \Gamma_i}{\|\hat{\mathbf{v}}_k\|\|\Gamma_i\|}\right)\right) \tag{18}$$

where the weight is controlled by plane error $E_{p,k}$ in (14).

Prior information in the MAP framework typically includes the ideal property of estimate. Planckian locus is adopted as a prior of illuminant. The possible illuminants in the real world are commonly well-represented by black body radiators. In chromaticity space, black body radiators make a locus according to the varying temperature, which is called Planckian locus [22, 28]. A candidate illuminant is orthogonally projected into Planckian locus on the CIE 1960 uv chromaticity space, and its Euclidean distance is converted into the prior probability as follows

$$p(\Gamma_i) = \exp\left(-\frac{d_{uv}(\Gamma_i)}{\lambda_b}\right) \tag{19}$$

Table 1. Angular error comparisons with various single image methods for specular video (150 fps).

Method		Mean	Median	Trimean	Best-25%	Worst-25%
Statistics-based	Gray world	4.87	4.50	5.46	2.22	8.26
	Max-RGB [24]	16.42	15.14	17.40	9.65	24.45
	Shades of gray [15]	5.11	3.39	6.92	2.09	10.87
	1^{st} order grey edge [43]	9.51	9.24	11.35	2.42	17.88
	2^{nd} order grey edge [43]	14.27	14.94	16.11	5.15	23.91
	Grey pixels [47]	7.99	6.98	9.03	4.58	13.20
Gamut-based	Pixel gamut [16]	8.19	8.06	9.00	3.84	13.31
	1^{st} order gradient gamut [18]	6.39	5.82	7.11	3.18	10.63
	2^{nd} order gradient gamut [18]	7.84	8.18	8.53	3.30	11.72
Physics-based	IIC [38]	7.22	6.91	7.87	3.73	11.39
	CLS [25]	9.01	8.55	10.12	3.48	15.39
	ICC [46]	3.78	2.15	6.61	0.79	10.12
	Proposed	2.47	1.93	3.12	0.50	5.12

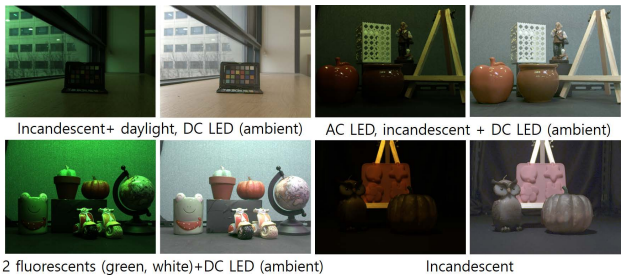

Figure 8. Visual results of the proposed method with various light sources.

where λ_b is a smoothing parameter, and $d_{uv}(\Gamma_i)$ is Euclidean projection distance between Γ_i and Planckian locus on CIE 1960 uv chromaticity space.

We aim to find a optimal illuminant which minimizes the MAP estimation of (17) from candidate illuminants. It is worth noting that λ_b controls the importance between likelihood and prior.

4. Experimental Results

To evaluate the proposed method, we produced 80 high-speed raw videos, which were captured using Sentech STC-MCS43U3V high-speed vision camera. Exposure time is set to half the number of frames per second, which is usually used (*e.g.* 1/150 sec for 75 fps). Each raw frame is normalized and demosaiced to apply color constancy. To convince that the proposed method works well irrespective of the amount of specularity, the test video sequences are categorized into specular (55% of total) and non-specular (45% of total) by the extent of specularity in videos. They are composed of various natural objects such as plastic, textile, metal, rubber, stones, and fruit (see Fig. 6). We regularly select 60 AC pixels among all to estimate a dichromatic plane (N_p=60). The ground truth chromaticity of illuminant is calculated by averaging the chromaticities of the reference white of a color checker. Angular error e is used to evaluate the quantitative performance and is given by

$$e = \arccos\left(\frac{\Gamma_g \cdot \hat{\Gamma}}{\|\Gamma_g\| \left\|\hat{\Gamma}\right\|}\right) \tag{20}$$

where Γ_g is a ground truth chromaticity.

Performance with Frame Rate To capture the fast AC variations of illuminant, the capture frame rate should exceed the frequency of illuminant. To avoid aliasing, it should be twice the Nyquist frequency for the case of unknown f_{ac} [27, 32]. However, it can be configured below the Nyquist frequency under the assumption of known f_{ac}. Fig. 7 (a) shows the angular error accuracy with various fps. When the frame rate is lower then 100 fps, the angular error of the proposed method is rather high because the variation of illuminant intensity becomes indistinguishable by insufficient number of samples. When the frame rate is over 100, the performance of the proposed method increased rapidly. We can see that the angular error performance is saturated when the frame rate is over 200 fps, which is still below the Nyquist frequency (240 Hz).

Fig. 7 (b) shows the angular error of the proposed method with the number of temporal observations. With the number of temporal observation, the accuracy of the proposed method increases until saturated. Note that the 15 temporal observations are made for 0.1 sec with 150 fps.

Comparisons with Single Image Methods To represent the video performance of single image methods, we sampled 10 frames from video regularly. Then, their angular errors are averaged to represent a video performance. Since an uniform AC light source is considered, our experimental setup is wrapped up with matte cloth to avoid the effect of external ambient light. The number of temporal observations is 100, which is less than 1 sec. We compare the proposed method to several state-of-the-art methods including

Table 2. Angular error comparisons with various single image methods for non-specular video (150 fps).

Method		Mean	Median	Trimean	Best-25%	Worst-25%
Statistics-based	Gray world	4.20	3.24	4.99	1.61	8.16
	Max-RGB [24]	11.76	12.27	12.86	5.22	18.51
	Shades of gray [15]	3.82	2.92	4.60	1.47	7.25
	1^{st} order grey edge [43]	4.07	2.69	5.68	1.34	9.03
	2^{nd} order grey edge [43]	5.43	3.86	7.35	2.17	11.80
	Grey pixels [47]	6.32	5.79	6.75	3.76	9.51
Gamut-based	Pixel gamut [16]	6.75	5.67	8.16	1.89	13.19
	1^{st} order gradient gamut [18]	11.74	12.58	12.46	6.59	15.85
	2^{nd} order gradient gamut [18]	12.37	12.76	12.72	8.41	15.63
Physics-based	IIC [38]	9.03	8.22	9.95	4.47	14.47
	CLS [25]	9.01	6.20	11.26	2.60	18.43
	ICC [46]	4.16	3.68	5.40	1.06	8.18
	Proposed	2.58	2.37	3.00	0.94	4.60

statistics-based, gamut-based, and physics-based methods. We classify our test videos into specular and non-specular videos, and evaluate each separately. Table 1 and 2 compare the proposed method with existing color constancy methods for a single image. The proposed method outperforms all existing methods. Especially, the performance of the proposed method is outstanding with worst-25% angular error, which is almost half of the second best methods. Compared to existing methods, the proposed method works well with specular as well as non-specular image.

Comparisons with Temporal Method The proposed method is compared with existing temporal method, which is dichromatic model in (4) (introduced in [31,48]). To conduct fair comparisons, 60 identical pixels are used, and principal component analysis is exploited to estimate illuminant in temporal method of (4). Table 3 summarizes the angular error performance of the proposed method. The proposed method shows the lower angular error, which is attributed to noise-robust characteristics of the proposed method.

Evaluation with various light sources We evaluate the proposed method with various combinations of light sources (as shown in Fig. 8) and the public DELIGHT [37]. Our fitting model in (6) are applied to both our experiment setting and DELIGHT. For evaluation with DELIGHT, its bulb response values are resampled to 60 Hz (originally 50 Hz). Note that the amplitude of sinusoidal variations are normalized to 1 for fair comparison. Table 4 shows that our model in (6) is well-fit to both data, independent of bulb types. Visual results of the proposed method are evaluated as shown in Fig. 8. With various environments under mixed AC light or ambient light, the proposed method works well.

5. Conclusions

We proposed a novel temporal color constancy method for AC light sources. Under AC light source, the intensities of a pixel (named by AC pixel) is time-varying with a frequency identical to AC electric power. This periodic time-varying property helps a dichromatic plane to be estimated accurately. A variety of experiments show that the proposed method can estimate an illuminant accurately, leading to better color constancy. Also, the proposed method outperforms existing dichromatic based methods and temporal color constancy methods, irrespective of the amount of specularity. In this paper, only a static scene is considered for experiments in order to avoid the effect of object motion. It would be possible to compensate motion by alignment between neighboring frames. It may take some time to acquire temporal pixel samples for dichromatic plane estimation, and this may be constrained by fast object motion. Higher speed capability can decrease the time length of AC pixels, resulting in less sensitive to object motion. It will be further investigated thoroughly.

Table 3. Angular error comparisons with temporal method for high-speed video (150 fps).

	Specular		Non-specular	
Method	Mean	Median	Mean	Median
Temporal	5.42	5.02	6.55	3.94
Proposed	2.47	1.93	2.58	2.37

Table 4. Mean squared error of our fitting method with DELIGHT dataset (top) and our experiment setting (bottom).

Data	Incan	Fluor	LED
DELIGHT	0.00001	0.00013	0.00045
Ours	0.00026	0.00047	0.00021

6. Acknowledgment

This work is supported by Samsung Electronics, and the National Research Foundation of Korea (NRF) grant funded by the Korea government (MSIT) (No. 2019R1A2C1005834).

References

[1] Kobus Barnard, Vlad Cardei, and Brian Funt. A comparison of computational color constancy algorithms. i: Methodology and experiments with synthesized data. *IEEE transactions on Image Processing*, 11(9):972–984, 2002.

[2] Jonathan T Barron. Convolutional color constancy. In *Proceedings of the IEEE International Conference on Computer Vision*, pages 379–387, 2015.

[3] Jonathan T. Barron and Yun-Ta Tsai. Fast fourier color constancy. In *The IEEE Conference on Computer Vision and Pattern Recognition (CVPR)*, July 2017.

[4] Simone Bianco, Claudio Cusano, and Raimondo Schettini. Single and multiple illuminant estimation using convolutional neural networks. *IEEE Transactions on Image Processing*, 26(9):4347–4362, 2017.

[5] Jacopo Bonato, Luigi M Gratton, Pasquale Onorato, and Stefano Oss. Using high speed smartphone cameras and video analysis techniques to teach mechanical wave physics. *Physics Education*, 52(4):045017, 2017.

[6] David H Brainard and William T Freeman. Bayesian color constancy. *JOSA A*, 14(7):1393–1411, 1997.

[7] Gershon Buchsbaum. A spatial processor model for object colour perception. *Journal of the Franklin institute*, 310(1):1–26, 1980.

[8] Ayan Chakrabarti. Color constancy by learning to predict chromaticity from luminance. In *Advances in Neural Information Processing Systems*, pages 163–171, 2015.

[9] Ayan Chakrabarti, Keigo Hirakawa, and Todd Zickler. Color constancy with spatio-spectral statistics. *IEEE Transactions on Pattern Analysis and Machine Intelligence*, 34(8):1509–1519, 2012.

[10] Marc Ebner. Color constancy based on local space average color. *Machine Vision and Applications*, 20(5):283–301, 2009.

[11] Graham D Finlayson and Steven D Hordley. Color constancy at a pixel. *JOSA A*, 18(2):253–264, 2001.

[12] Graham D Finlayson, Paul M Hubel, and Steven Hordley. Color by correlation. In *Color and Imaging Conference*, volume 1997, pages 6–11. Society for Imaging Science and Technology, 1997.

[13] Graham D Finlayson and Gerald Schaefer. Convex and non-convex illuminant constraints for dichromatic colour constancy. In *Computer Vision and Pattern Recognition, 2001. CVPR 2001. Proceedings of the 2001 IEEE Computer Society Conference on*, volume 1, pages I–I. IEEE, 2001.

[14] Graham D Finlayson and Gerald Schaefer. Solving for colour constancy using a constrained dichromatic reflection model. *International Journal of Computer Vision*, 42(3):127–144, 2001.

[15] Graham D Finlayson and Elisabetta Trezzi. Shades of gray and colour constancy. In *Color and Imaging Conference*, volume 2004, pages 37–41. Society for Imaging Science and Technology, 2004.

[16] David A Forsyth. A novel algorithm for color constancy. *International Journal of Computer Vision*, 5(1):5–35, 1990.

[17] Arjan Gijsenij and Theo Gevers. Color constancy using natural image statistics and scene semantics. *IEEE Transactions on Pattern Analysis and Machine Intelligence*, 33(4):687–698, 2011.

[18] Arjan Gijsenij, Theo Gevers, and Joost Van De Weijer. Generalized gamut mapping using image derivative structures for color constancy. *International Journal of Computer Vision*, 86(2-3):127–139, 2010.

[19] Arjan Gijsenij, Theo Gevers, Joost Van De Weijer, et al. Computational color constancy: Survey and experiments. *IEEE Transactions on Image Processing*, 20(9):2475–2489, 2011.

[20] David John Griffiths. *Developmemt of High Speed High Dynamic Range Videography*. PhD thesis, Virginia Tech, 2017.

[21] Yuanming Hu, Baoyuan Wang, and Stephen Lin. Fc4: Fully convolutional color constancy with confidence-weighted pooling. In *The IEEE Conference on Computer Vision and Pattern Recognition (CVPR)*, July 2017.

[22] Deane B Judd, David L MacAdam, Günter Wyszecki, HW Budde, HR Condit, ST Henderson, and JL Simonds. Spectral distribution of typical daylight as a function of correlated color temperature. *Josa*, 54(8):1031–1040, 1964.

[23] Johann Heinrich Lambert. *Photometria sive de mensura et gradibus luminis, colorum et umbrae*. Klett, 1760.

[24] Edwin H Land. The retinex theory of color vision. *Scientific american*, 237(6):108–129, 1977.

[25] Thomas M Lehmann and Christoph Palm. Color line search for illuminant estimation in real-world scenes. *JOSA A*, 18(11):2679–2691, 2001.

[26] Laurence T Maloney and Brian A Wandell. Color constancy: a method for recovering surface spectral reflectance. In *Readings in Computer Vision*, pages 293–297. Elsevier, 1987.

[27] Mrinal Mandal and Amir Asif. *Continuous and Discrete Time Signals and Systems with CD-ROM*. Cambridge University Press, 2007.

[28] Baptiste Mazin, Julie Delon, and Yann Gousseau. Estimation of illuminants from projections on the planckian locus. *IEEE Transactions on Image Processing*, 24(6):1944–1955, 2015.

[29] John J McCann, Suzanne P McKee, and Thomas H Taylor. Quantitative studies in retinex theory a comparison between theoretical predictions and observer responses to the color mondrian experiments. *Vision research*, 16(5):445–IN3, 1976.

[30] Christa Neumeyer. On perceived colors. *Behavioral and Brain Sciences*, 15(1):49–49, 1992.

[31] Veronique Prinet, Dani Lischinski, and Michael Werman. Illuminant chromaticity from image sequences. In *Proceedings of the IEEE International Conference on Computer Vision*, pages 3320–3327, 2013.

[32] John G Proakis. *Digital signal processing: principles algorithms and applications*. Pearson Education India, 2001.

[33] Yanlin Qian, Ke Chen, Jarno Nikkanen, Joni-Kristian Kamarainen, and Jiri Matas. Recurrent colour constancy. In *Proc. IEEE Int. Conf. on Computer Vision (ICCV), Venice, Italy, 22–29 October 2017*, 2017.

[34] Yanlin Qian, Ke Chen, Jarno Nikkanen, Joni-Kristian Kämäräinen, and Jiri Matas. Dichromatic gray pixel for camera-agnostic color constancy. *arXiv preprint arXiv:1803.08326*, 2018.

[35] Gerald Schaefer. Robust dichromatic colour constancy. In *International Conference Image Analysis and Recognition*, pages 257–264. Springer, 2004.

[36] Steven A Shafer. Using color to separate reflection components. *Color Research & Application*, 10(4):210–218, 1985.

[37] Mark Sheinin, Yoav Y Schechner, and Kiriakos N Kutulakos. Computational imaging on the electric grid. In *Proceedings of the IEEE Conference on Computer Vision and Pattern Recognition*, pages 6437–6446, 2017.

[38] Robby T Tan, Katsushi Ikeuchi, and Ko Nishino. Color constancy through inverse-intensity chromaticity space. In *Digitally Archiving Cultural Objects*, pages 323–351. Springer, 2008.

[39] Shoji Tominaga and Brian A Wandell. Natural scene-illuminant estimation using the sensor correlation. *Proceedings of the IEEE*, 90(1):42–56, 2002.

[40] Javier Toro. Dichromatic illumination estimation without pre-segmentation. *Pattern Recognition Letters*, 29(7):871–877, 2008.

[41] Javier Toro and Brian Funt. A multilinear constraint on dichromatic planes for illumination estimation. *IEEE Transactions on Image Processing*, 16(1):92–97, 2007.

[42] Joost Van De Weijer and Shida Beigpour. The dichromatic reflection model-future research directions and applications.

[43] Joost Van De Weijer, Theo Gevers, and Arjan Gijsenij. Edge-based color constancy. *IEEE Transactions on image processing*, 16(9):2207–2214, 2007.

[44] Michael Vollmer and Klaus-Peter Möllmann. Flickering lamps. *European Journal of Physics*, 36(3):035027, 2015.

[45] PÅ Wedin. On the gauss-newton method for the nonlinear least-squares problems. *Institute for Applied Mathematics, Stockolm, Sweden, Working Paper*, 24, 1974.

[46] Sung-Min Woo, Sang-Ho Lee, Jun-Sang Yoo, and Jong-Ok Kim. Improving color constancy in an ambient light environment using the phong reflection model. *IEEE Transactions on Image Processing*, 27(4):1862–1877, 2018.

[47] Kai-Fu Yang, Shao-Bing Gao, and Yong-Jie Li. Efficient illuminant estimation for color constancy using grey pixels. In *Proceedings of the IEEE Conference on Computer Vision and Pattern Recognition*, pages 2254–2263, 2015.

[48] Qingxiong Yang, Shengnan Wang, Narendra Ahuja, and Ruigang Yang. A uniform framework for estimating illumination chromaticity, correspondence, and specular reflection. *IEEE Transactions on Image Processing*, 20(1):53–63, 2011.